

2. Principle of Operation and Proposed Control Scheme

According to the above studies, current mode and voltage mode controller are suitable for current source section and voltage source section, respectively. It is noticeable that the limitation is originated from the feedback loop gain. In the SAS engine, the control reference signal is generated by the SAS output variable and it will define the outer feedback loop gain, which converts from the sensed signal to the reference signal. For example, the outer feedback gain is determined by the incremental slope of the I-to-V conversion LUT in the voltage mode control or that of the V-to-I conversion LUT in the current mode control. However, if the feedback gain is extremely reduced beyond their operating region as shown in Fig.3 (a), where the system becomes unstable and shows the poor dynamic response.

Our main research object is to develop a universal control scheme that extends the control range to the entire range of I-V curve in a simple and numerically stable manner. Impedance based control can be a viable solution to alleviate the problem caused by too small outer loop gain, the impedance mapping can be done as shown in Fig. 3 (b). It reflects that distinct reference values can be generated by impedance feedback. However, according to our observation, this method has a practical issue near the open circuit condition and short circuit condition. The measured impedance usually becomes either too large in the voltage source segment or too small in the current source segment. Near open circuit condition, the impedance reaches to extremely large value (near infinity) and system stability can be lost. A similar issue is occurred near short circuit condition when the impedance is approaching zero. Thus, our study answers to this issue by shifting the origin point as shown in Fig. 3 (c). The formation of the

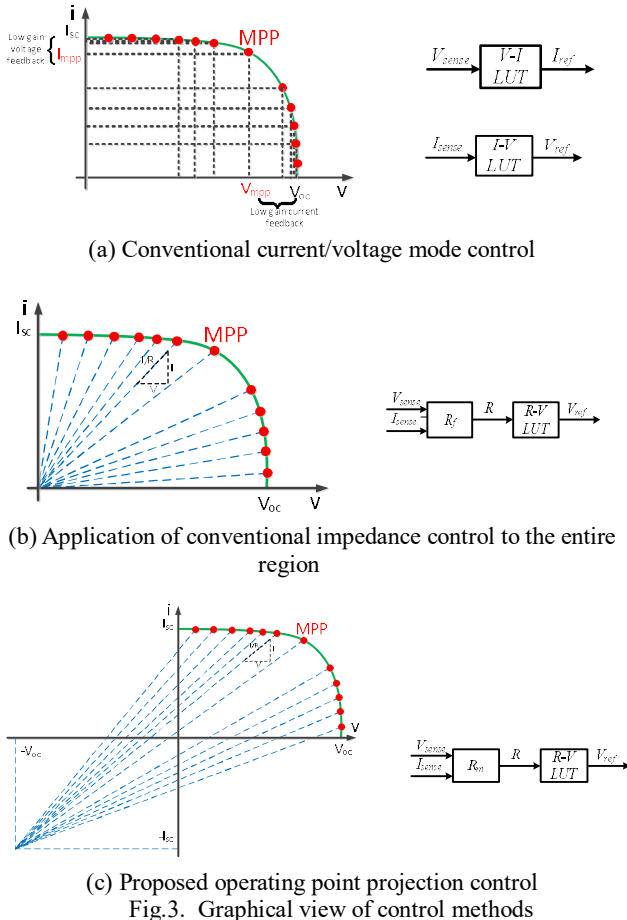


Fig.3. Graphical view of control methods

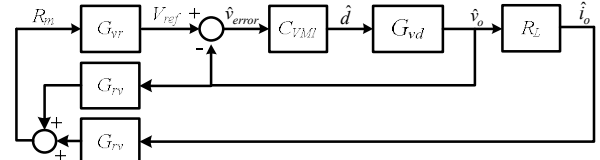


Fig.4. Small signal block diagram

modified impedance R_m is derived using (2).

$$R_m = \frac{V_{sense} + V_{oc}}{I_{sense} + I_{sc}} \quad (2)$$

where, V_{oc} is the open circuit and I_{sc} is the short circuit current in the standard test condition (STC). The shifting by V_{oc} and I_{sc} makes the feedback gain to be confined into a finite region that never become zero or infinity. This technique guarantees appropriate outer feedback gain to have stable operation in the entire I-V curve.

In the proposed scheme, the R-to-V conversion LUT is used to generate the reference voltage. The system small signal block diagram is shown in Fig. 4. Consequently, the LUT is developed according to the R_m . The voltage transfer function is derived as (3). The compensator can be designed considering the inner voltage loop (G_{vd}) and the outer loop gain. Transfer functions of voltage and current into resistance and R_m are defined (4), (5), and (6), respectively. Mathematical stability analysis and design procedure will be included in the full paper.

$$G_{vd}(s) = \frac{\hat{v}_o(s)}{\hat{d}(s)} \quad (3)$$

$$G_{rv} = \frac{\hat{r}_m}{\hat{v}_o} \quad (4)$$

$$G_{ri} = \frac{\hat{r}_m}{\hat{i}_o} \quad (5)$$

$$G_{vr} = \frac{\hat{v}_{ref}}{\hat{r}_m} \quad (6)$$

3. Performance Verification

To verify the performance of the proposed solar panel simulator, the simulation and hardware are implemented, and results are shown in Table 1. The system specifications are shown in Table 2. The system is tested on $1000W/m^2$ insulations and $25^\circ C$ temperature. The schematic as shown in Fig.7 is used in the simulation and different loads are changed in 0.07th second in PSIM. Simulation waveforms of output voltage and current in the transience of $RL=10\Omega \rightarrow 20\Omega$ is shown in Fig. 8. V_o , I_o , and R_m are observed with the result of error around 1.2%.

The experiment is performed with a buck power converter and resistive loads as shown in Fig. 9. The SAS controller and SAS engine are implanted in a DSP. Load resistance is changed from 10Ω to 20Ω , and the waveforms of output voltage and current, voltage input of ACD in DSP, and the duty of buck converter are presented in Fig. 10. In the experiments, two active loads are parallel connected, and one load is activated after few seconds to obtain the transient. Numerical experiment results are also shown in Table 1 with the error below 3.5%. The accuracy of simulation and experiment has a slight difference because of noise. The proposed system settles the output value within 0.02s with very low oscillation. These results prove that the proposed scheme could able to follow the datasheet values successfully and

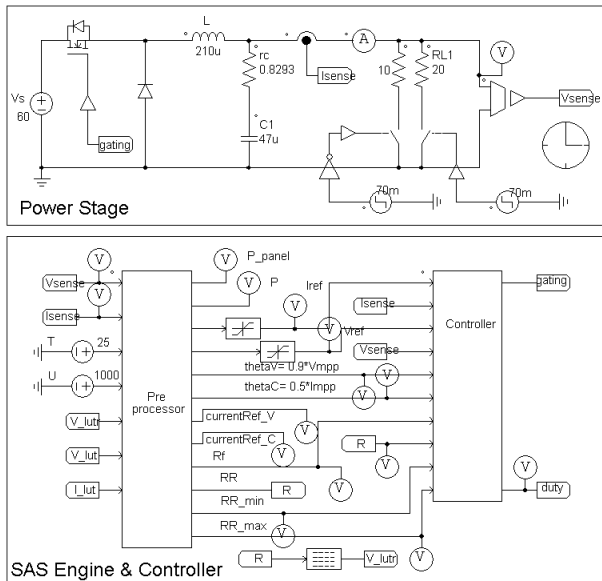


Fig.5. Solar Array Simulator using PSIM

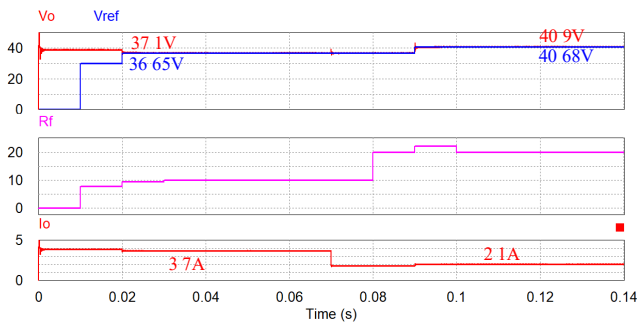


Fig.6. Simulation of RL=10Ω→20Ω transient

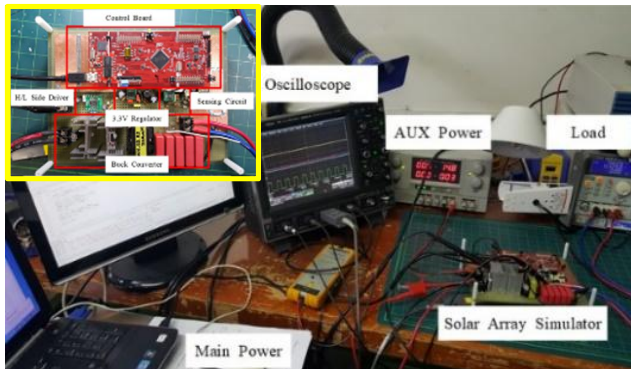


Fig.7. Experimental setup of solar array

performs enough speed and stability.

4. Conclusion

In this paper, a universal control scheme for the solar panel simulator is designed, analyzed and verified. To solve the stability problem of the conventional works, it utilizes an operating point projection technique to construct an R-to-V conversion LUT. The proposed scheme adopts a single controller with impedance feedback. The modified impedance is calculated by the operating point projection formula to have a finite outer feedback gain. The controller is designed by using the small-signal modeling and the system stability is mathematically analyzed. The simulation and experiment results show that control stability and response speed

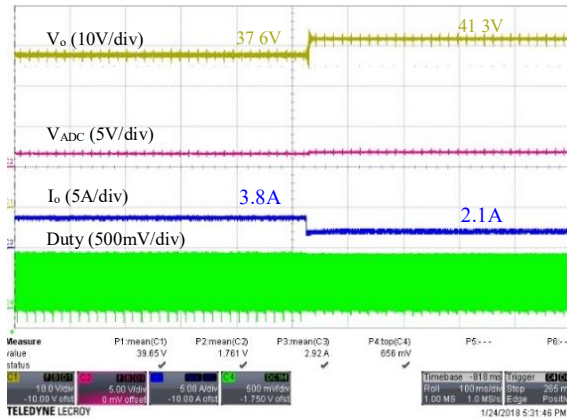


Fig.8. Experiment result of load change

of the solar array simulator are verified through real hardware implementation. In the final paper, detailed mathematical descriptions of the outer loop stability improvements and more hardware test results in the presence of maximum power point trackers will be included.

References

- [1] D. Sera, R. Teodorescu, and P. Rodriguez, "PV Panel Model Based on Datasheet Values," IEEE International Symposium on Industrial Electronics, pp. 2392-2396, 2007.
- [2] Shlomo Gadelovits, Moshe Sitbon and Alon Kuperman, "Rapid Prototyping of a Low-Cost Solar Array Simulator Using an Off-the-Shelf DC Power Supply," IEEE Transactions on Power Electronics, Vol.29, NO.10, Oct.2014
- [3] A.Vijayakumari, A.T.Devarajan and N.Devarajan, "Design and development of a model-based hardware simulator for photovoltaic array," Electrical Power & Energy Systems, 43(2012), p.40-46
- [4] Y. Li, T. Lee, F. Z. Peng and D. Liu, "A Hybrid Control Strategy for Photovoltaic Simulator," 2009 24th Annual IEEE Applied Power Electronics Conf. and Expo., Washington, DC, 2009, pp. 899-903.
- [5] I.D.G. Jayawardana, C.N.M. Ho, M. Pokharel, and G. Escobar, "A fast dynamic photovoltaic simulator with instantaneous output impedance matching controller," 2017 IEEE Energy Conversion Congress and Exposition (ECCE), pp.5126 – 5132, 2017